LETTER

doi:10.1038/nature10437

Molecular organization of vomeronasal chemoreception

Yoh Isogai[1,2], Sheng Si[1], Lorena Pont-Lezica[1]†, Taralyn Tan[1], Vikrant Kapoor[1], Venkatesh N. Murthy[1] & Catherine Dulac[1,2]

The vomeronasal organ (VNO) has a key role in mediating the social and defensive responses of many terrestrial vertebrates to species- and sex-specific chemosignals[1]. More than 250 putative pheromone receptors have been identified in the mouse VNO[2,3], but the nature of the signals detected by individual VNO receptors has not yet been elucidated. To gain insight into the molecular logic of VNO detection leading to mating, aggression or defensive responses, we sought to uncover the response profiles of individual vomeronasal receptors to a wide range of animal cues. Here we describe the repertoire of behaviourally and physiologically relevant stimuli detected by a large number of individual vomeronasal receptors in mice, and define a global map of vomeronasal signal detection. We demonstrate that the two classes (V1R and V2R) of vomeronasal receptors use fundamentally different strategies to encode chemosensory information, and that distinct receptor subfamilies have evolved towards the specific recognition of certain animal groups or chemical structures. The association of large subsets of vomeronasal receptors with cognate, ethologically and physiologically relevant stimuli establishes the molecular foundation of vomeronasal information coding, and opens new avenues for further investigating the neural mechanisms underlying behaviour specificity.

The discovery of large receptor families mediating olfactory and vomeronasal chemosensation has offered a unique opportunity to decode the molecular logic by which environmental information influences animal behaviour[3,4]. The VNO of rodents has a critical role in identifying sex- and species-specific chemical cues and in mediating mating, territorial aggression, defensive responses to predators and associated endocrine changes[1,5]. With rare exceptions[6–8], the molecular identity of VNO receptors (VRs) recognizing distinct animal cues is unknown, thus limiting the ability to explore the sensory mechanisms underlying behavioural specificity. Prior studies suggested that vomeronasal detection is extremely sensitive and narrowly tuned to male, female or heterospecific cues[5,9–11], but they have not allowed the identification of the activated receptors. We describe here a robust and high-throughput molecular readout of vomeronasal activation that enabled us to uncover the receptor specificity of 88 individual VRs to a vast range of ethologically relevant cues. These results establish the molecular and functional framework underlying vomeronasal signalling.

In initial experiments, we exposed female mice to clean bedding and to bedding used by male mice, and assessed the upregulation of the immediate early genes (IEGs) *Arc*, *c-Fos*, *c-Jun*, *Egr1*, *FosB* and *Nr4a1* by *in situ* hybridization on VNO tissue. Our data show that the sensitivity of *Egr1* induction following exposure to chemosignals far exceeds that of other IEGs (Fig. 1a, b) (60.1 ± 7.1 cells per $0.2\,mm^2$ for *Egr1*, 7.9 ± 1.9 cells per $0.2\,mm^2$ for *c-Fos*). Indeed *c-Fos*, an IEG used in previous VNO stimulation studies, labels only a subset of *Egr1*-positive cells (Supplementary Fig. 1). In $TrpC2^{-/-}$ mutants, in which VNO activation is genetically impaired[12], *Egr1* induction after semiochemical exposure is completely abolished ($n = 3$), demonstrating the specificity of *Egr1* activation following sensory stimulation (Fig. 1c).

We then exposed animals to 29 distinct ethologically relevant cues[5,13]. Male and female bedding from different mouse subspecies and wild-derived strains, as well as a variety of heterospecific cues from sympatric competitors and predators, robustly induced *Egr1* expression in the VNO (Fig. 2a). Remarkably, food-related insect stimuli and cues from presumably neutral species such as woodchuck failed to generate VNO activation.

V1R and V2R neurons were equally activated by a large variety of stimuli, as judged by co-labelling of *Egr1* with $G\alpha_{i2}$, a marker of V1R-expressing neurons[14,15] (Fig. 2b, Supplementary Fig. 2a). Interestingly, simultaneous exposure to multiple cues from the same class of animals (for example, *Peromyscus* species, reptiles, or predatory birds) did not significantly increase the number of *Egr1*-positive cells when compared to activation by a single stimulus ($P > 0.4$, two-tailed *t*-test when the strongest of each stimulus class was compared to the corresponding mix), indicating that neuronal populations activated by related animals are largely overlapping (Fig. 2a). In contrast, simultaneous exposure to all heterospecific stimuli significantly increased *Egr1*-positive cells from 5% to 10% per cue to up to ~30% ($P < 0.01$, two-tailed *t*-test), indicating that distinct heterospecific cues have different response profiles. Moreover, whereas mouse bedding activated 5% to 7% of VNO neurons in animals of the opposite sex, mixes of conspecific and heterospecific scents activated ~35% of neurons (Fig. 2a), suggesting that receptors activated by both types of cues are also largely distinct.

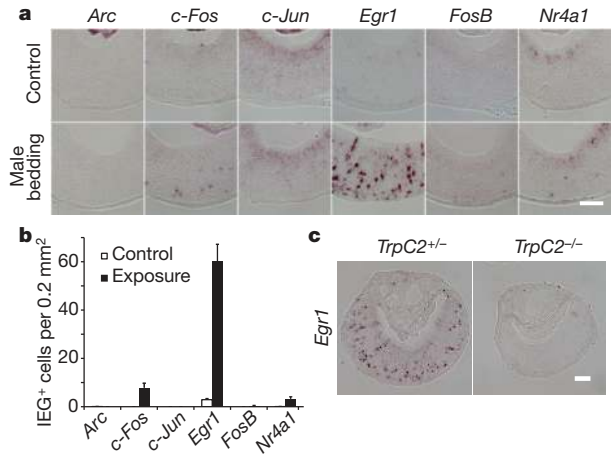

Figure 1 | *Egr1* expression is robustly induced by pheromone-evoked VNO neuronal activation. Female CD-1 mice were exposed to clean or male mouse bedding and their VNOs analysed for expression of various immediate early genes (IEGs). **a**, *In situ* hybridization with RNA probes to *Arc*, *c-Fos*, *c-Jun*, *Egr1*, *FosB* and *Nr4a1*. **b**, Numbers of IEG-positive cells after bedding exposure (10 sections per VNO, $n = 3$ animals). Error bars, s.e.m. **c**, TrpC2, a cation channel involved in VNO signal transduction is required for *Egr1* induction. Female $TrpC2^{+/-}$ or $TrpC2^{-/-}$ mice were exposed to male conspecific bedding and *Egr1* expression was visualized in the VNO. Scale bar, 100 μm.

[1]Department of Molecular and Cellular Biology, Center for Brain Science, Harvard University, Cambridge, Massachusetts 02138, USA. [2]Howard Hughes Medical Institute, Department of Molecular and Cellular Biology, Center for Brain Science, Harvard University, Cambridge, Massachusetts 02138, USA. †Present address: Ecole Normale Supérieure, Paris 75005, France.

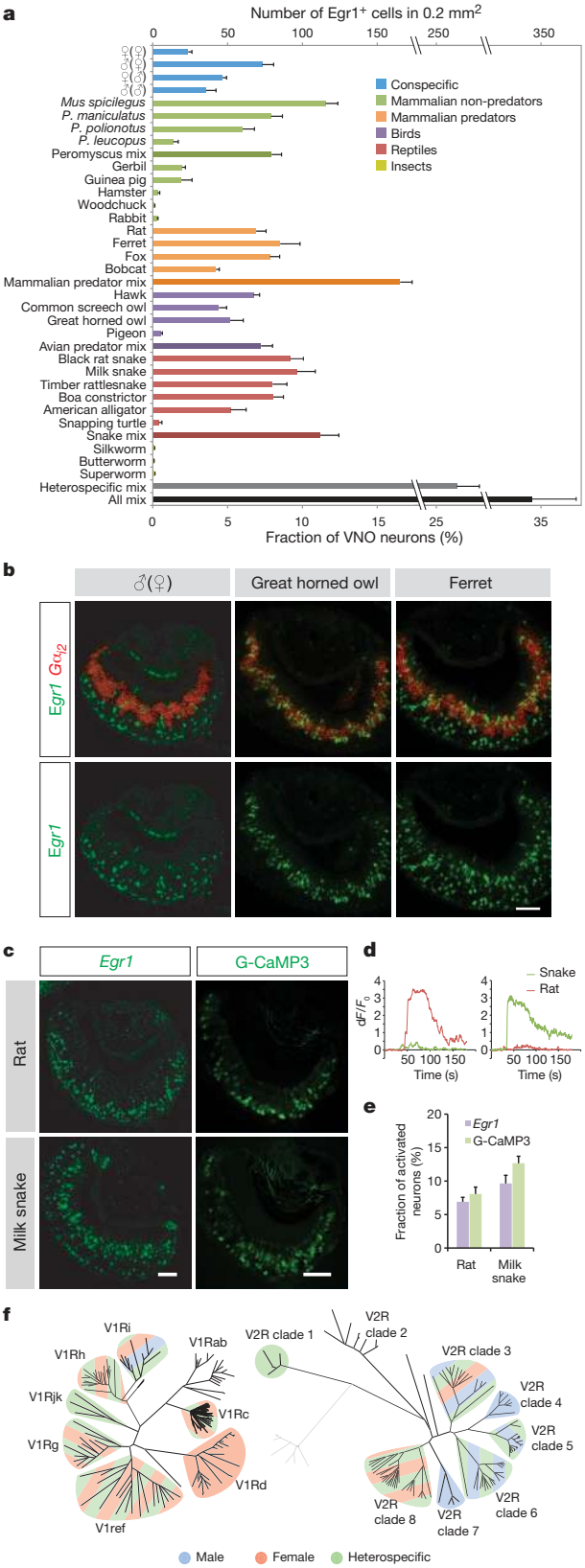

Figure 2 | Widespread activation of VNO receptors by conspecific and heterospecific cues. **a**, Survey of ethologically relevant vomeronasal stimuli. Vomeronasal neural activation on exposure to conspecific and heterospecific cues was visualized by *Egr1* induction and quantified. Detection of female cues by males is designated as ♀(♂). Unless specified, female mice were used. Mixed heterospecific cues activated *Egr1* in significantly more cells than individual stimuli ($P < 0.01$, two-tailed *t*-test). Co-exposure to heterospecific and conspecific stimuli (all mix, $n = 6$) resulted in significantly more *Egr1*-positive cells ($P < 0.05$, two-tailed *t*-test). **b**, Widespread activation of VNO neurons by conspecific and heterospecific cues. Shown are *in situ* hybridization results with probes against $G\alpha_{i2}$ (red) and *Egr1* (green). **c**, Comparison between *Egr1* and G-CaMP3-evoked signal in response to rat or milk snake chemosignals. G-CaMP3 images are 10-s averages of ΔF frames within stimulus period. **d**, Differential response profiles of neurons to rat or snake signals. Stimuli were perfused from 20 s to 60 s. **e**, Quantitative comparison between *Egr1* and G-CaMP3-evoked signals. The percentage of activated cells identified by G-CaMP3 ($n = 356$ cells for rat stimuli, $n = 566$ cells for snake stimuli, 9 VNO slices from 3 animals) among those responsive to 40 mM KCl was plotted in the graph. Data for *Egr1* were taken from **a**. The difference between *Egr1* and G-CaMP3 was not statistically significant ($P > 0.1$, two tailed *t*-test). **f**, Clade-level maps of V1R (left) and V2R (right) activation show distinct clade specificity for male, female or heterospecific cues. Hatched patterns indicate response to multiple types of cues. Error bars, s.e.m. Scale bars, 100 μm.

To assess *Egr1* as a readout of VNO activation, we compared it to cue-evoked neuronal responses visualized by the genetically encoded calcium indicator, G-CaMP3 (ref. 16). Strikingly, *Egr1* and G-CaMP3 reported remarkably similar patterns of activities in the basal, or basal-plus-apical VNO neuroepithelium following exposure to rat and snake stimuli, respectively (Fig. 2c–e), confirming *Egr1* induction as an exquisitely sensitive and accurate marker of VNO neuronal activation.

Next, we developed a high-throughput platform to uncover the receptors activated by specific cues. With the exception of widely expressed V2R2 receptors[17], vomeronasal neurons are thought to express a unique receptor gene from the V1Rs or V2Rs. We generated 209 RNA probes that specifically identify individual or subgroups of VRs by *in situ* hybridization. A collection of clade-specific probes was designed to target all receptor sequences within each of the eight distinct V1R or V2R clades (Fig. 2f). Probes with higher specificity that readily distinguish a single or few closely related VR sequences were designed on the basis of divergent 5′-UTR/intron[18] and 3′-UTR regions in VR genes. The specificity of these probes for closely related VRs was validated by dual colour *in situ* hybridization (Supplementary Fig. 3). Although detecting all VRs at single gene resolution was technically impossible, our probes targeted 139 distinct VRs with a specificity of a single (or at most a few) gene.

We then used a hierarchical approach to systematically uncover VRs activated by distinct cues (Supplementary Figs 2b, 4). First, the co-expression of *Egr1* with either $G\alpha_{i2}$, $G\alpha_o$ or formyl peptide receptors (FPRs)[19,20] identified the nature of the activated neurons as expressing a V1R, V2R or FPR, respectively. Most stimuli activated both V1R- and V2R-expressing neurons, while a few activated only V1R- (hawk and owls) or V2R-expressing cells (rat, fox and male mouse cues in females) (Supplementary Table 1). We found no activation of FPR-expressing cells. We then assessed the specific V1R or V2R clades associated with the activated neurons (Fig. 2f, Supplementary Fig. 2c). Interestingly, some clades appeared specifically stimulated by a distinct class of cues, for example, V1Rd and V2R clades 4 and 7 by sex-specific cues. Subsequently, receptor specific probes were used to unmask the exact molecular identity of the *Egr1*-positive cells. By collecting data from 9,948 VNO slices, each containing approximately 1,000 neurons, we succeeded in the identification of 88 receptors (56 V1Rs and 32 V2Rs, 78 single and 10 unresolved receptors) associated with distinct cues (Supplementary Fig. 5, Supplementary Table 1, 2). Importantly, these receptors span most V1R and V2R clades, thus generating the most comprehensive functional map of vomeronasal receptors to date.

The vomeronasal system plays an essential part in regulating sex-specific behaviours. Previous reports suggest that vomeronasal neurons detect sex-specific cues in mouse urine, tear and saliva[9,10,13,21,22], and Vmn2r116 (or V2Rp5) was identified as detecting the male pheromone ESP1 (ref. 6; Supplementary Fig. 6). Our strategy uncovered 28 receptors (25 single, 3 unresolved) detecting mouse cues, among which 26 detecting sex-specific cues (Fig. 3a–c, Supplementary Table 1). Only two receptors (V1ri9, V1ri10) responded to both male and female mouse cues, consistent with the desensitization of IEG induction *in*

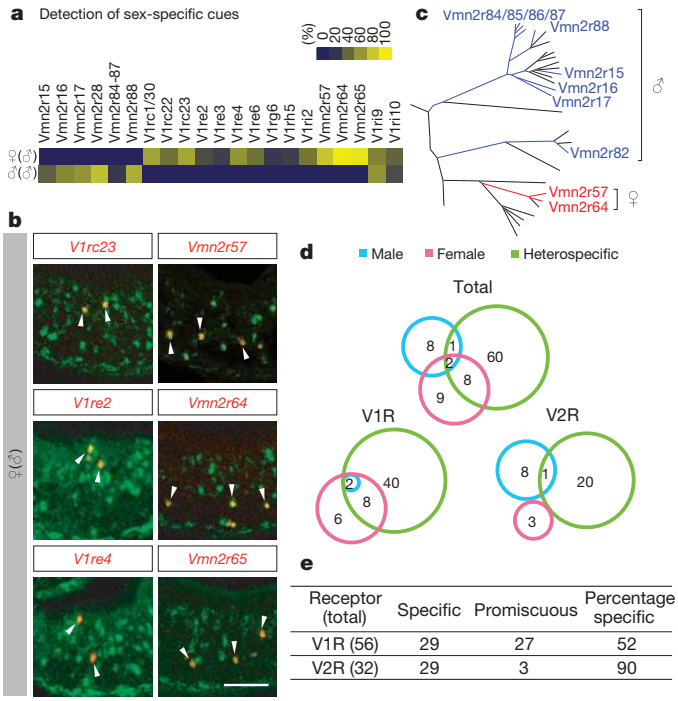

Figure 3 | Receptor responses to sex-specific cues. **a**, **b**, Male and female mouse cues are each detected by a specific subset of V1Rs and V2Rs. **a**, Heat maps representing the co-localization between *Egr1* and representative vomeronasal receptor genes (yellow, 100% overlap; dark blue, 0% overlap). **b**, *In situ* hybridization of *Egr1* (green) and individual receptors (red), with arrows marking co-localization of *Egr1* and receptor signals. Scale bars, 100 μm. **c**, Clade organization of V2Rs detecting male (blue) or female (red) cues. **d**, Receptors detecting male (blue), female (red) and heterospecific (green) cues are largely distinct. **e**, V1Rs and V2Rs display distinct specificity. Shown are the numbers of receptors that detect unique types of cues (specific) versus multiple types (promiscuous) among the following categories: male, female, mammalian non-predator, mammalian predator, reptile, and avian predator.

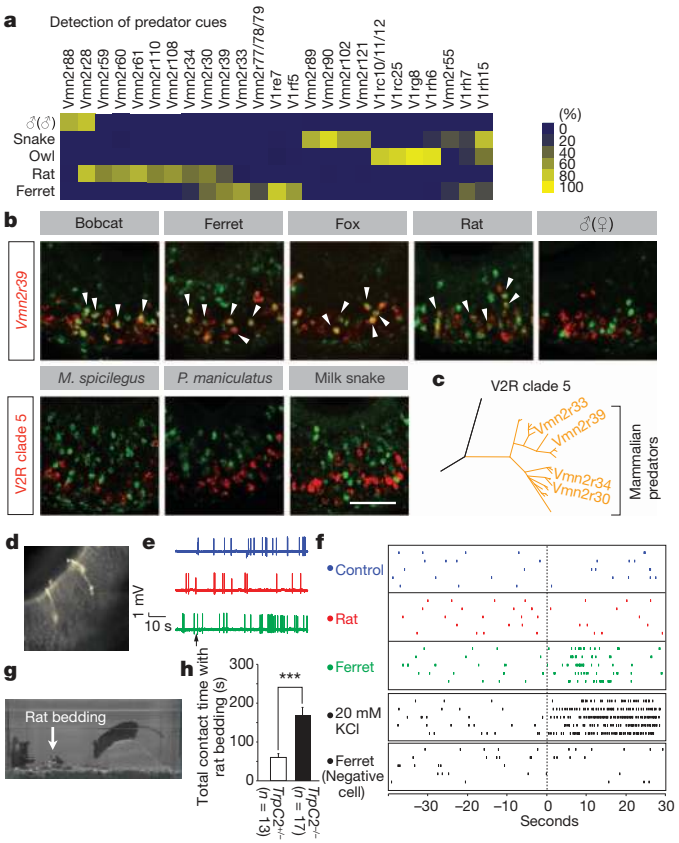

Figure 4 | Receptor responses to heterospecific cues. **a**, **b**, Predator cues are detected by a specific subset of V1Rs and V2Rs. **a**, Heat map representing the co-localization between *Egr1* and representative vomeronasal receptor genes (colour coding as Fig. 3a). **b**, *In situ* hybridization of *Egr1* (green) and vomeronasal receptors (red), with arrows marking co-localization of *Egr1* and receptor signals. Scale bar, 100 μm. **b**, **c**, Mammalian predator cues commonly activate V2R clade 5 receptors. Owing to high homology among V2R clade 5 genes, the *Vmn2r30*, *33*, *34*, *39* probes detect multiple receptors. **d**, Fluorescence image showing a patched V1rh7-YFP neuron. **e**, Loose-patch recordings of a V1rh7-YFP neuron. The arrow indicates perfusion start. **f**, Spike raster for three different VNO neurons, showing responses of a V1rh7-YFP neuron to ferret, but not to rat stimuli, and no response of a V1Rh7-YFP-negative neuron to ferret stimuli. The stimulus perfusion started at −30 s and lasted 20 s. **g**, **h**, Rat bedding (arrow) elicits robust avoidance behaviours in control $TrpC2^{+/-}$ mice, but significantly less in $TrpC2^{-/-}$ mice lacking VNO activity. $***P < 0.0001$ (two-tailed Student's *t*-test). Error bars, s.e.m. ($TrpC2^{+/-}$, $n = 13$; $TrpC2^{-/-}$, $n = 17$).

vivo by self-secreted stimuli[6]. Four receptors (V1re2, V1re3, V1re6, V1rg6) were selectively activated by female cues in males and females, while a larger set of V1Rs and V2Rs responded to female cues only in males (Fig. 3a–c, Supplementary Table 1). In addition, responses to male-specific signals involved Vmn2r116, Vmn2r28, Vmn2r15, Vmn2r16 and Vmn2r17 in males and females, Vmn2r66 and Vmn2r82 in females, and Vmn2r84/85/86/87 and Vmn2r88 in males (Fig. 3a–c, Supplementary Table 1). Interestingly, no V1R was found to specifically respond to male cues. Thus, consistent with a previous report[9], the detection of sex-specific cues appears to rely on a small and specific subset of VNO neurons, the identity of which is now clearly established. This molecular logic is likely to underlie the initiation of sex-dependent behavioural interactions, such as male–male aggression and mating behaviours.

Vomeronasal detection of heterospecific cues, or kairomones, is involved in adaptive defensive behaviours[5,13,23]. Indeed, rat bedding induces robust avoidance to the predator cues in $TrpC2^{+/-}$ but not in $TrpC2^{-/-}$ animals (Fig. 4g, h). Moreover, $TrpC2^{-/-}$ animals exhibited abnormal ingestive behaviour of the predator bedding, suggesting that VNO inputs also inhibit foraging[24,25] (Supplementary Fig. 7).

We report here the identity of 71 (63 single, 8 unresolved) receptors activated by heterospecific scents. Consistent with the distinct behavioural outputs generated by pheromones and kairomones, we found that only 11 receptors were common to both types of cues, whereas 60 were uniquely activated by heterospecific stimuli, and 17 by mouse cues only (Fig. 3d). The detection of kairomones thus emerges as a major function of the VNO[5,13]. The identity of one of the identified receptor population for the detection of predator cues was confirmed independently by *Egr1* activation in cells expressing YFP under the V1Rh7 promoter[26] (Supplementary Fig. 8). Further, loose patch recording of V1Rh7-YFP expressing neurons demonstrated significant increase in firing rates following exposure to ferret, but not to rat stimuli (1.732 ± 0.170 Hz for ferret, 0.420 ± 0.061 Hz for rat, $n = 4$) (Fig. 4d–f, Supplementary Fig. 9).

Remarkably, some receptors show unique association with distinct classes of predators. Vmn2r89 and Vmn2r121 were exclusively activated by scents from snakes, V1rc10/11/12 by owls. Also, up to 70% of V2R clade 5 neurons were activated by every mammalian predator tested, but not by sympatric non-predators (Fig. 4a–c, Supplementary Fig. 5, 10). Moreover, each predator cue generated a distinct receptor signature: for example, rat stimuli activate Vmn2r59, Vmn2r60, Vmn2r61, Vmn2r108 and Vmn2r110, all within clade 8, whereas ferret cues activate V1rf5 and Vmn2r77/78/79, suggesting that the mouse VNO has the sensory machinery to discriminate predator species.

We then searched for receptors detecting the sympatric species *Mus spicilegus* and *Mus musculus*, which diverged evolutionarily ~1.5 million years ago and do not breed in the wild[27,28]. Receptors activated by *M. spicilegus* and *M. musculus* male cues appear mostly distinct, though often closely related (Supplementary Figs 5, 11). For

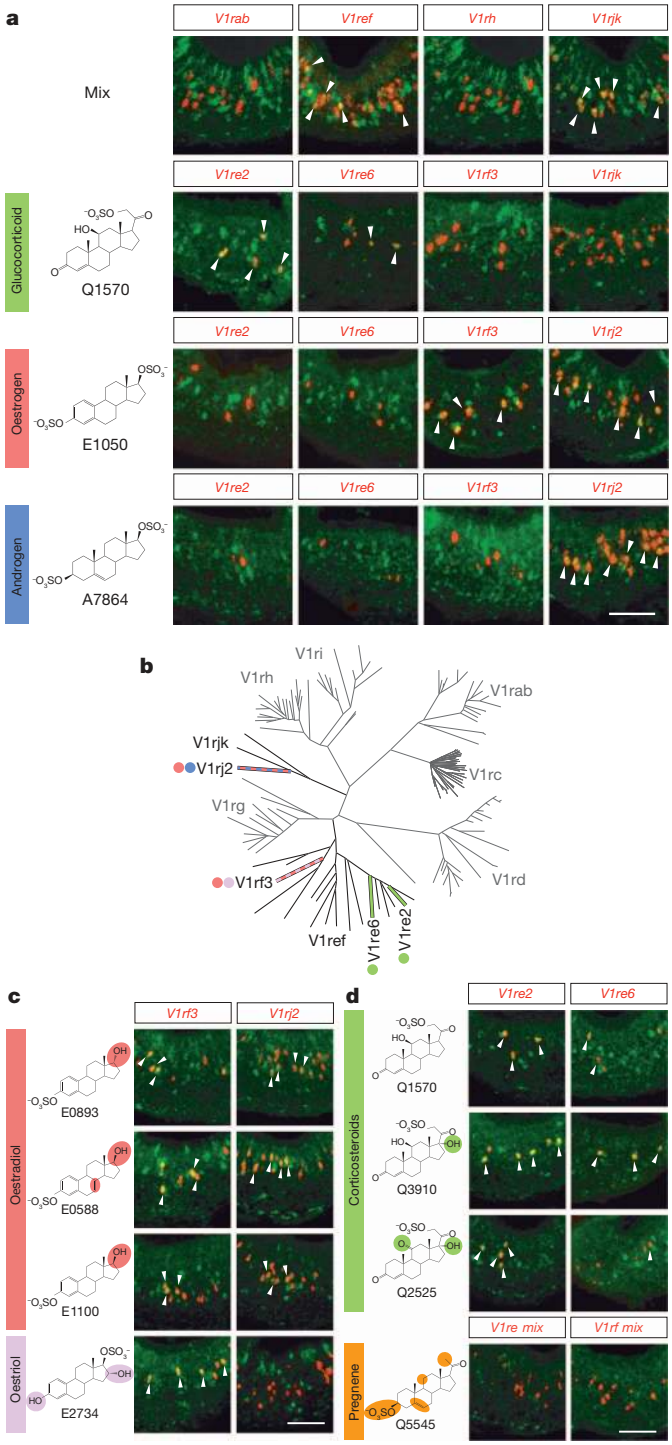

Figure 5 | Sulphated steroids detection by V1Rs. **a**, V1Ref and V1Rjk clade-specific probes (red) co-localize with *Egr1* (green) after VNO stimulation by a mix of steroids containing glucocorticoids such as Q1570 (green), oestrogens such as E1050 (red) and androgens such as A7864 (blue). Each of these compounds on its own elicits activity in distinct populations of vomeronasal neurons (V1re2, V1re6, V1rf3 and V1rj2), also represented in the molecular tree of V1R receptors (**b**). Specific receptors detecting each steroid are indicated by dots, using the same colour scheme as **a** and **c**. **c**, The three distinct oestradiols (red) activate both V1rf3 and V1rj2 whereas the oestriol (purple) only activates V1rf3. **d**, The sulphate group position in pregnenes (corticosteroids in green, pregnenolone in orange) determines the specificity of ligand detection by V1re2 and V1re6. Differences in chemical structures among tested compounds are highlighted by coloured circles. Arrowheads mark co-localization between *Egr1* and receptor signals. Scale bar, 100 μm.

example, Vmn2r8/9 and Vmn2r11, activated by *M. spicilegus*, and Vmn2r15, Vmn2r16 and Vmn2r17, activated by *M. musculus*, belong to clade 6 (Supplementary Fig. 11b). Likewise, Vmn2r69 (activated by *M. spicilegus*) and Vmn2r66 (activated by *M. musculus*) belong to clade 3. Thus, through the activation of specialized receptors, *M. musculus* may readily discriminate scents emitted by closely related but reproductively incompatible species, a property that could be linked to the reproductive isolation of these species.

V1Rs and V2Rs are associated with segregated neural pathways[29], raising the possibility that fundamental functional differences may exist between the two families. Remarkably, our data suggest that V1Rs and V2Rs display different receptor properties. Nearly half of the V1Rs (27 out of 56) exhibit generalized activation by multiple cues (Fig. 3e), including signals with apparent conflicting behavioural significance. For example, receptors within the V1Rh, V1Rc and V1Re clades were activated by mouse, predator and non-predator cues (Supplementary Tables 1 and 2, Supplementary Fig. 12). In contrast, most V2Rs (29 out of 32) are activated by cues reflecting a unique ethological context such as a male, a female, or a given type of predator or non-predator. In addition, hierarchical clustering across all identified receptors revealed clear segregation between V1Rs and V2Rs (Supplementary Fig. 5). These results suggest that V1R and V2R pathways may encode different types of information: individual V2Rs appear uniquely poised to encode information about the identity of emitters with clear behavioural significance—for example, the sex of a conspecific or the nature (predator or competitor) of a heterospecific. In contrast, individual V1Rs may encode other forms of biologically relevant information.

To gain further insight into the molecular logic of V1R-mediated signalling, we investigated the detection of sulphated steroids, which are thought to account for 80% of VNO neuronal activation by female urine[30] (probably through V1Rs[11]). Our data show that, when male mice were exposed to a mix of synthetic steroid sulphates, receptors from V1Ref and V1Rjk clades were specifically activated (Fig. 5a, b). We then tested individual compounds to attempt the pairing of specific steroid ligands with their cognate receptors. Corticosterone-21 sulphate (Q1570), a compound in female urine[30], strongly activated V1re2 and more weakly V1re6 cells (Fig. 5a, b). Both receptors were shown in earlier experiments to be specifically activated by female cues (Fig. 3a). In addition, we uncovered strong activation of V1rf3 by 17β-oestradiol sulphate (E1050) and V1rj2 by both E1050 and 5-androstene-3β, 17β-diol disulphate (A7864) (Fig. 5a), although these two receptors were not activated by female bedding, indicating that these steroids are not secreted under normal conditions.

Thus, our approach efficiently achieved single compound resolution, offering the unique opportunity to test the receptor specificity to a variety of individual chemicals. We further tested four sulphated oestrogen compounds structurally related to E1050, and three additional sulphated pregnenes structurally related to Q1570. V1rf3 appeared broadly selective to oestradiols, oestriols and related stereoisomers, regardless of sulphate positions, but did not respond to androgens or glucocorticoids (Fig. 5c). Interestingly, no other V1rf receptor was activated by these ligands. In contrast, V1rj2 was activated by androgens and oestradiols but not oestriols. Similarly, V1re2 and V1re6 selectively detected corticosteroids (Fig. 5d). Therefore, V1R receptors can distinguish distinct structural classes of steroids. Androgens, oestrogens and glucocorticoids are ubiquitous though sensitive reporters of the animal endocrine state. Our results thus suggest that V1Rs may serve as detectors of the physiological status of an animal.

In conclusion, our data have begun to uncover the molecular logic by which vomeronasal receptors of different families, clades and receptor sequences extract biological information and trigger appropriate behavioural responses to animals of a given sex, species and physiological status. The collection of receptors uncovered in this study provides a molecular foundation to further dissect the neural circuits governing social and sexual communication in rodents.

METHODS SUMMARY

Stimulus exposure was conducted by introducing a subject animal (male or female CD-1 mice, 8 to 14 weeks old) in a fresh cage containing distinct animal cues for 30 min (for Fig. 1) or 40 min (for Figs 2–5). The dissected VNOs were embedded in OCT (Tissue-Tek) and frozen in dry ice. Cryosections (16 μm) of VNO were subjected to RNA *in situ* hybridization using IEG and VR probes.

Full Methods and any associated references are available in the online version of the paper at www.nature.com/nature.

Received 13 January; accepted 8 August 2011.
Published online 21 September 2011.

1. Dulac, C. & Torello, A. T. Molecular detection of pheromone signals in mammals: from genes to behaviour. *Nature Rev. Neurosci.* **4,** 551–562 (2003).
2. Zhang, X., Marcucci, F. & Firestein, S. High-throughput microarray detection of vomeronasal receptor gene expression in rodents. *Front. Neuroscience* **4,** 164 (2010).
3. Dulac, C. & Axel, R. A novel family of genes encoding putative pheromone receptors in mammals. *Cell* **83,** 195–206 (1995).
4. Buck, L. & Axel, R. A novel multigene family may encode odorant receptors: a molecular basis for odor recognition. *Cell* **65,** 175–187 (1991).
5. Papes, F., Logan, D. W. & Stowers, L. The vomeronasal organ mediates interspecies defensive behaviors through detection of protein pheromone homologs. *Cell* **141,** 692–703 (2010).
6. Haga, S. *et al.* The male mouse pheromone ESP1 enhances female sexual receptive behaviour through a specific vomeronasal receptor. *Nature* **466,** 118–122 (2010).
7. Leinders-Zufall, T., Ishii, T., Mombaerts, P., Zufall, F. & Boehm, T. Structural requirements for the activation of vomeronasal sensory neurons by MHC peptides. *Nature Neurosci.* **12,** 1551–1558 (2009).
8. Boschat, C. *et al.* Pheromone detection mediated by a V1r vomeronasal receptor. *Nature Neurosci.* **5,** 1261–1262 (2002).
9. He, J., Ma, L., Kim, S., Nakai, J. & Yu, C. R. Encoding gender and individual information in the mouse vomeronasal organ. *Science* **320,** 535–538 (2008).
10. Leinders-Zufall, T. *et al.* Ultrasensitive pheromone detection by mammalian vomeronasal neurons. *Nature* **405,** 792–796 (2000).
11. Holekamp, T. F., Turaga, D. & Holy, T. E. Fast three-dimensional fluorescence imaging of activity in neural populations by objective-coupled planar illumination microscopy. *Neuron* **57,** 661–672 (2008).
12. Stowers, L., Holy, T. E., Meister, M., Dulac, C. & Koentges, G. Loss of sex discrimination and male-male aggression in mice deficient for TRP2. *Science* **295,** 1493–1500 (2002).
13. Ben-Shaul, Y., Katz, L. C., Mooney, R. & Dulac, C. *In vivo* vomeronasal stimulation reveals sensory encoding of conspecific and allospecific cues by the mouse accessory olfactory bulb. *Proc. Natl Acad. Sci. USA* **107,** 5172–5177 (2010).
14. Berghard, A. & Buck, L. B. Sensory transduction in vomeronasal neurons: evidence for $G\alpha_o$, $G\alpha_{i2}$, and adenylyl cyclase II as major components of a pheromone signaling cascade. *J. Neurosci.* **16,** 909–918 (1996).
15. Jia, C. & Halpern, M. Subclasses of vomeronasal receptor neurons: differential expression of G proteins ($G\alpha_{i2}$ and $G\alpha_o$) and segregated projections to the accessory olfactory bulb. *Brain Res.* **719,** 117–128 (1996).
16. Tian, L. *et al.* Imaging neural activity in worms, flies and mice with improved GCaMP calcium indicators. *Nature Methods* **6,** 875–881 (2009).
17. Martini, S., Silvotti, L., Shirazi, A., Ryba, N. J. & Tirindelli, R. Co-expression of putative pheromone receptors in the sensory neurons of the vomeronasal organ. *J. Neurosci.* **21,** 843–848 (2001).
18. Stewart, R. & Lane, R. P. V1R promoters are well conserved and exhibit common putative regulatory motifs. *BMC Genomics* **8,** 253 (2007).
19. Liberles, S. D. *et al.* Formyl peptide receptors are candidate chemosensory receptors in the vomeronasal organ. *Proc. Natl Acad. Sci. USA* **106,** 9842–9847 (2009).
20. Rivière, S., Challet, L., Fluegge, D., Spehr, M. & Rodriguez, I. Formyl peptide receptor-like proteins are a novel family of vomeronasal chemosensors. *Nature* **459,** 574–577 (2009).
21. Holy, T. E., Dulac, C. & Meister, M. Responses of vomeronasal neurons to natural stimuli. *Science* **289,** 1569–1572 (2000).
22. Taha, M., McMillon, R., Napier, A. & Wekesa, K. S. Extracts from salivary glands stimulate aggression and inositol-1, 4, 5-triphosphate (IP3) production in the vomeronasal organ of mice. *Physiol. Behav.* **98,** 147–155 (2009).
23. Samuelsen, C. L. & Meredith, M. The vomeronasal organ is required for the male mouse medial amygdala response to chemical-communication signals, as assessed by immediate early gene expression. *Neuroscience* **164,** 1468–1476 (2009).
24. Brown, J., Kotler, B., Smith, R. & Wirtz, W. The effects of owl predation on the foraging behavior of heteromyid rodents. *Oecologia* **76,** 408–415 (1988).
25. Sundell, J. *et al.* Variation in predation risk and vole feeding behaviour: a field test of the risk allocation hypothesis. *Oecologia* **139,** 157–162 (2004).
26. Wagner, S., Gresser, A. L., Torello, A. T. & Dulac, C. A multireceptor genetic approach uncovers an ordered integration of VNO sensory inputs in the accessory olfactory bulb. *Neuron* **50,** 697–709 (2006).
27. Chevret, P., Veyrunes, F. & Britton-Davidian, J. Molecular phylogeny of the genus Mus (Rodentia: Murinae) based on mitochondrial and nuclear data. *Biol. J. Linn. Soc.* **84,** 417–427 (2005).
28. Guénet, J. L. & Bonhomme, F. Wild mice: an ever-increasing contribution to a popular mammalian model. *Trends Genet.* **19,** 24–31 (2003).
29. Dulac, C. & Wagner, S. Genetic analysis of brain circuits underlying pheromone signaling. *Annu. Rev. Genet.* **40,** 449–467 (2006).
30. Nodari, F. *et al.* Sulfated steroids as natural ligands of mouse pheromone-sensing neurons. *J. Neurosci.* **28,** 6407–6418 (2008).

Supplementary Information is linked to the online version of the paper at www.nature.com/nature.

Acknowledgements We acknowledge H. Fisher, H. Hoekstra, E. Kay, M. Kirchgessner, N. Uchida, A. Wang, X.-D. Wang, B. Watson, W. Tong, Harvard Museum of Natural History, Harvard Concord Field Station, Museum of Science, Boston, and New England Wildlife Center, for providing stimulus materials used in this study, L. Looger for the G-CaMP3 construct, M. Wienisch, F. Markopoulos and D. Mak for help with electrophysiology and imaging experiments, and B. Goetze and the Harvard Center for Biological Imaging for help with microscopy. We also thank members of the Dulac laboratory for critical reading of the manuscript, S. Andreeva for technical support and R. Hellmiss for help with figure artwork. This work was supported by the NIDCD at the National Institute of Health, the Howard Hughes Medical Institute and the Damon Runyon Cancer Research Foundation (Y.I., DRG-1981-08).

Author Contributions Y.I. and C.D. designed the study. Y.I., S.S. and T.T. designed and generated RNA probes, performed RNA *in situ* hybridization, and analysed data. L.P.-L. performed pilot experiments for data shown in Fig. 1 and produced recombinant ESP1. Y.I. and V.K. performed calcium imaging and electrophysiology. V.N.M. supervised physiology experiments. Y.I. and C.D. wrote the paper.

Author Information Reprints and permissions information is available at www.nature.com/reprints. The authors declare no competing financial interests. Readers are welcome to comment on the online version of this article at www.nature.com/nature. Correspondence and requests for materials should be addressed to C.D. (dulac@fas.harvard.edu).

METHODS

Sampling of animal stimuli. Bedding materials used in this study were all freshly sampled from cages that house live animals (Harvard University, Harvard Museum of Natural History, Harvard Concord Field Station, Tufts University, Museum of Science, Boston, and New England Wildlife Center). Soiled bedding represents the most complete stimulus source for animals, and is also of ecological relevance. Bedding materials typically absorb a wide range of chemical stimuli excreted by animals, such as urine, faeces, saliva, fur, and other gland secretions. Since different animals are housed in different environments, we flexibly adjusted the sampling procedures. For instance, chemosignals emitted by heterospecific mammals and birds (male rat, female fox, male ferret, female bobcat, male *Peromyscus*, male *M. spicilegus*, male and female gerbils, male and female hamsters, male and female rabbits, woodchuck, pigeon, red tailed hawk, screech owl, and great horned owl) were sampled as soiled bedding (paper, woodchips or corn cob). For reptiles, we sampled faeces, urate and other gland secretions absorbed in woodchips or paper. These bedding materials were directly used for exposure experiments (as described separately below). For aquatic animals such as alligators, only faecal pellets were sampled. For insect larvae, live animals were directly used for exposure experiments. Some predators such as snake and predatory birds were fed mice as part of their diet, and we took great care to avoid potential odour contamination. For example, on bedding sampling we avoided areas where mouse carcass was present in animal cages. Second, to sample milk snake odour, which we extensively used for our study, we changed bedding after the feeding to avoid potential odour contamination from mice. We also tested materials from multiple individuals whenever possible. Judging from the number of *Egr1*-positive cells, we did not find extensive individual variability in these samples. If multiple individuals were not available, especially for bobcat, hawk and great horned owl, we tested stimulus samples from different collection dates. We stored these bedding materials at 4 °C for the short term (one week) and at −20 °C for the long term. These materials, even after long term storage at −20 °C when the amount of volatiles was significantly reduced, did not appreciably lose their ability to robustly stimulate vomeronasal neurons.

For conspecific stimuli, to represent a potential diversity of chemical cues emitted by different subspecies of mice, we collected bedding samples from 5 different strains of mice: BALB/c (Jackson Labs), PWD/PhJ (Jackson Labs), CAST/EiJ (Jackson Labs), Idaho[31] and Chuuk[31], and exposed these samples as a mixture. It is known that mice secrete different vomeronasal cues reflecting their physiological states, for example, different phases of oestrous[9], prompting us to sample materials freshly from cages that house multiple animals over 1 week. Thus, conspecific stimuli used in our study probably contain chemosignals secreted over different phases of the oestrous cycles. We stored these materials at 4 °C for the short term and −20 °C for the long term.

Stimulus exposure. For most exposure experiments involving bedding stimuli, approximately 50 ml (in volume) of bedding containing animal cues were placed in a clean cage. We introduced a subject mouse (male or female CD-1, from 8 weeks to 14 weeks old, Charles River), which voluntarily made extensive direct contacts with introduced stimuli in freely behaving conditions. The animals were exposed to stimuli for 30 min (for Fig. 1) or 40 min (for Figs 2–5). Subsequently, the dissected VNOs were embedded in OCT (Tissue-Tek) and frozen in dry ice. VNO cryosections (16 μm) were used for RNA *in situ* hybridization using IEG and vomeronasal receptor probes. Control experiments were conducted using fresh bedding in an identical manner. For insect larvae exposure, 3–4 insect larvae were directly introduced to the cages. For alligator stimuli, a few faecal pellets were used. For heterospecific mix exposure experiments, ~100 ml mixture of the following bedding sample was used: *Peromyscus* (*P. maniculatus, P. leucopus, P. polionotus*), mammalian predators (bobcat, fox, ferret, rat), avian predators (screech owl, great horned owl, red tail hawk), reptiles (rat snake, milk snake, rattlesnake, boa, alligator), and *M. spicilegus*. For pure chemicals such as ESP1 and sulphated steroids, ~5 μl of Ringer's (in mM; 115 NaCl, 5 KCl, 2 $CaCl_2$, 2 $MgCl_2$, 25 $NaHCO_3$ and 5 HEPES) containing the stimuli were directly spotted on each nostril. Recombinant ESP1 was purified as a GST fusion protein overexpressed in *Escherichia coli* using pET41 vector (Novagen), followed by thrombin cleavage to release the ESP1 peptide. 2 μg of the peptide was exposed to each animal.

Sulphated steroid exposure. Steroids were purchased from Steraloids. A mix of steroids (A6940, epitestosterone sodium sulphate; A7864, 5-androsten-3β, 17β-diol disulphate; E1050, 17β-oestradiol sulphate; E0893, 17α-oestradiol sulphate; P3817, allopregnanolone sulphate; P8200, epipregnanolone sulphate, Q1570, corticosterone 21-sulphate; Q3470, deoxycorticosterone 21-glucoside; each at 250 μM in Ringer's) were used for initial screens. Subsequently, individual steroids (Q1570; E1050; A7864; E0893; E0588, 17β-dihydroequilin 3-sodium sulphate; E1100, 17β-oestradiol 3-sulphate; E2734, oestriol 17-sulphate; Q3910, hydrocortisone 21-sodium sulphate; Q2525, cortisone 21-sulphate; Q5545, 3β-hydroxy-5-pregnen-20-one 3-sulphate) were used at 500 μM in Ringer's. 5 μl of steroid solution were spotted on each nostril of male CD-1 animals (8–14 weeks), and the animals were exposed to steroids for 40 min. Experiments were conducted for at least three animals.

Preparation of RNA probes. For immediate early gene probes, we have cloned complementary DNA of *Arc*, *c-Fos*, *c-Jun*, *Egr1*, *FosB* and *Nr4a1* in approximately 900-base-pair (bp) segments to pCRII-TOPO or pCR4-TOPO vector (Invitrogen). Antisense cRNA probes were synthesized using T3, T7 or Sp6 polymerases (Promega) and digoxigenin (DIG) or fluorescein (FITC) labelling mix (Roche) from PCR templates. All IEG probes consisted of a cocktail of 2–3 probes to cover nearly the full length of these messenger RNAs.

For V1R clade-specific probes, we cloned full length coding sequence of V1R receptors (V1rab: *V1ra1*, *a2*, *a3*, *a4*, *a5*, *a6*, *a7*, *a8*, *b1*, *b2*, *b7*, *b8*, *b9*; V1rc: *V1rc3*, *c8*, *c10*, *c16*, *c28*; V1rd: *V1rd6*, *d9*, *d11*, *d12*, *d14*, *d22*, *Vmn1r167*; V1ref: *V1re1*, *e2*, *e3*, *e4*, *e6*, *e7*, *e8*, *e9*, *e10*, *e11*, *e12*, *e13*, *Vmn1r224*, *f1*, *f2*, *f3*, *f4*, *f5*; V1rh: *V1rh1*, *h20*; V1ri: *V1ri1*, *i3*, *i4*, *i5*, *i6*, *i8*; V1rjk: *V1rj2*, *j3*, *k1*) and combined these probes to generate a clade-specific probe set. For V1rg receptors, ~1 kilobase (kb) 5′-UTR/intron sequences of the following genes were used: *V1rg1*, *g2*, *g3*, *g4*, *g5*, *g6*, *g7*, *g8*, *g9*, *g10*, *g11*, *g12*, *Vmn1r77*, which were combined with *V1rl* cDNA probe to generate the V1Rgl clade probe set.

To generate clade-specific V2R probes, we cloned the first ~900 bp of annotated V2R receptor coding sequence (V2R clade 1: *Vmn2r55*; V2R clade 2: *Vmn2r19*, *Vmn2r20*, *Vmn2r24*; V2R clade 3: *Vmn2r65*, *Vmn2r69*, *Vmn2r76*, *Vmn2r77*; V2R clade 4: *Vmn2r115*; V2R clade 5: *Vmn2r28*, *Vmn2r48*; V2R clade 6: *Vmn2r8*, *Vmn2r15*, *Vmn2r17*, *Vmn2r84*, *Vmn2r89*, *Vmn2r118*; V2R clade 7: *Vmn2r18*, *Vmn2r81*, *Vmn2r83*, *Vmn2r120*; V2R clade 8; *Vmn2r57* 3′UTR probe, *Vmn2r58*, *Vmn2r63*, *Vmn2r58*, *Vmn2r90*, *Vmn2r93*, *Vmn2r96*, *Vmn2r97*, *Vmn2r99*, *Vmn2r102*, *Vmn2r104*, *Vmn2r105*, *Vmn2r106*, *Vmn2r108*, *Vmn2r110*, and *Vmn2r64* 3′-UTR probe) and combined these probes to generate clade-specific probe sets. To generate cRNA probes specific to individual V1R genes, we cloned ~1 kb 5′-UTR intron sequence of V1R genes to pCRII vector (Invitrogen). To produce cRNA probes specific to individual V2R receptors, we cloned ~600 bp of V2R 3′-UTR segments. These RNA probes were first used to test mRNA expression. We found that some annotated vomeronasal receptor genes did not appear to be expressed, since these RNA probes gave no discernible signals. For all vomeronasal receptor genes, for which we could confirm the expression, we tested the specificity of these probes by dual colour *in situ* hybridization using DIG and FITC probes and used for receptor mapping experiments. Probes generated in our study to detect specific receptors are listed in Supplementary Table 1. The VR nomenclature was based on that of GenBank and Mouse Genome Informatics.

RNA *in situ* hybridization. Single colour RNA *in situ* hybridization was conducted essentially as described[32]. We used DIG labelled cRNA probes at 2 ng μl^{-1} and used a hybridization temperature of 65 °C for experiments shown in Fig. 1. For *Egr1 in situ* hybridization experiments shown in Fig. 2, we used 68 °C as the hybridization temperature. Dual colour fluorescence *in situ* hybridization was conducted in the following steps. First, the tissue was fixed in 4% formaldehyde/1× PBS for 10 min, and washed 3 times with 1× PBS for 3 min each. The tissues were treated with acetylation solution (0.1 M triethanolamine with 2.5 μl ml^{-1} acetic anhydride) for 10 min. After 3 washes with 1× PBS, each for 5 min, the slide was incubated with the pre-hybridization solution (50% formamide, 5× SSC, 5× Denhardt's, 2.5 mg ml^{-1} yeast RNA, 0.5 mg ml^{-1} herring sperm DNA) for 2 h. The hybridization buffer (4% dextran sulphate, Millipore, added to pre-hybridization buffer) containing FITC labelled *Egr1* probes (a cocktail of three probes, each at 50 pg μl^{-1}) and DIG labelled VR probes (at 0.5 ng μl^{-1} for cDNA probes, and 1 ng μl^{-1} for 5′-UTR-intron and 3′-UTR probes) was heated at 95 °C for 3 min and immediately chilled on ice for 5 min. The hybridization solution was applied to the slides, which were covered with parafilm and incubated in a sealed chamber for 16 h at 68 °C. Following hybridization, the slides were washed with 5× SSC once for 5 min, and with 0.2× SSC three times, each for 20 min at 68 °C. Slides were washed at room temperature with 0.2× SSC for 5 min and subsequently with TNT buffer (100 mM Tris, pH 7.5, 150 mM NaCl, 0.05% Tween 20) for 5 min.

After the post-hybridization washes, 200 μl of anti-FITC-POD (Roche, at 1/250 dilution in TNB blocking buffer, Perkin-Elmer) was applied and incubated for 3 h at room temperature. Slides were washed with TNT buffer for a total of 1 h, with buffer exchanges every 10 min. The signal was developed using the TSA biotin plus kit (Perkin Elmer), as per manufacturer's protocol. The slides were washed with TNT buffer 3 times, each for 5 min, and subsequently treated with 3% H_2O_2/1×PBS to kill residual peroxidase activity. Slides were washed again 3 times with 1× PBS and TNT, each for 5 min. DIG antibody solution (anti-DIG-POD, Roche, at 1/500 dilution, and Streptavidin-Alexa488, Invitrogen, at 1/250 dilution in TNB buffer) were applied to the slides and incubated overnight at 4 °C. After washing slides with TNT (6 times, 10 min each), the signal was developed using the TSA

Cy3 plus kit (Perkin Elmer) as per manufacturer's protocol. Slides were washed with TNT (3 times, 5 min each and once for 1 h), and tissues were mounted with Vectashield (Vector labs) containing 8 μg ml^{-1} DAPI. All the microscopy images were acquired using LSM510 or AxioImager Z2 (Zeiss).

Analysis of *in situ* hybridization images. For single colour *in situ* hybridization images, quantitation was conducted using a minimum of 10 VNO sections per animal and 3 animals (data in Fig. 1) or 3–4 animals (data in Fig. 2). Since we found that 0.2 mm^2 represents areas occupied by medial cryostat sections of the VNO and contain approximately 1,000 VNO cells, we used the average number of *Egr1*-positive cells per 0.2 mm^2 in Fig. 1, and we converted these numbers to percentage of activated neurons among total VNO neurons in Fig. 2. For dual colour *in situ* hybridization, we quantitated the co-localization of *Egr1* and receptor signals over four sections per VNO, for a minimum of three animals. We then calculated the percentage of activated neurons in specific receptor neurons, for each odour class, and generated a co-localization matrix. In many cases, we found that individual receptor mapping is unnecessary when the hierarchical screen can unequivocally demonstrate that there are no activated neurons in specific receptor clades. In these cases, we input zero values to the co-localization matrix. For hierarchical clustering of the co-localization matrix, we used the Cluster program (http://bonsai.hgc.jp/~mdehoon/software/cluster/software.htm), with average linkage in Euclidian distance. To generate the clustering diagram in Supplementary Fig. 4, we calculated the average number of receptor neurons per receptor in 12 sections and used this as a weight. The heat map and clustering dendrogram were generated using the Java Treeview program (http://jtreeview.sourceforge.net/).

Behavioural assay. Male *TrpC2* mice (+/− or −/−, 8–14 weeks old, ref. 12) were single-housed three days before the experiment in a manner blind to the experimenter. The behaviour experiment was conducted by introducing 50 ml volume of fresh or rat bedding to one side of the cage, away from the nest area. The behaviours of the subject mice were video recorded and total contact time as well as ingestive behaviour were scored by an individual blind to the genotype. We defined ingestive behaviour as animals engaged in ingestion while holding a food pellet with two forepaws.

Generation of OMP-GCaMP3 transgenic line. pJOMP plasmid containing the rat olfactory marker protein (OMP) genomic sequence[33] was modified so that the G-CaMP3 ORF sequence completely replaces the OMP ORF. Linearized vector was used for pronuclear injection (performed by Harvard Genome Modification Facility), and transgenic founders were further backcrossed to C57Bl/6 mice to establish an OMP-GCaMP3 line. This line expresses the transgene uniformly throughout the vomeronasal epithelium and showed no sign of reported cell toxicity[15].

Calcium imaging on VNO slices. Calcium imaging was carried out essentially as described[9], using 5–8-week-old female OMP-GCaMP3 mice. The VNOs were acutely dissected, separated from bones, and embedded in 4% low melting point agar in mACSF (in mM; 130 NaCl, 5 KCl, 1 $MgCl_2$, 2.5 $CaCl_2$, 1.25 NaH_2PO_4, 25 $NaHCO_3$, 10 glucose). The coronal vibratome sections (200 μm) were cut, and slices were kept in continuously oxygenated mACSF for up to 8 h at 25 °C. The flow rate of the stimulus was approximately 0.3 ml min^{-1}, and we delivered stimulus for 40 s. All imaging was conducted at 25 °C. The fluorescence changes due to calcium transients were monitored using a LSM710 microscope with a GaAsP detector (Zeiss). We used a 1:100 dilution of freshly sampled rat urine from 2–6-month-old CD male rats (Charles River) in mACSF. For snake stimuli, shredded snake bedding (that is, paper) was extracted with mACSF, filtered and used for stimulation. To quantify the number of activated cells, we first generated ΔF images by subtracting an average of 20 s frames corresponding to initial resting period from the raw images. We then created an average ΔF image consisting of 10 s frames corresponding to the maximum fluorescence interval (shown in Fig. 2c). This operation significantly reduced the fluorescence signals from spontaneous activity, which is typically short (lasting 1–2 s) and consists of small bursts, and enriched evoked activity, which is a more sustained (more than 10 s), larger rise in fluorescent intensity. The fluorescence traces of individual positive cells were further examined to confirm the sustained nature of the response. The number of activated cells was quantified using ImageJ. To quantify the number of viable cells during the imaging experiments, we counted the number of G-CaMP3-positive cells responsive to 40 mM KCl in mACSF.

Electrophysiology. Loose patch recordings were performed at room temperature with a Multiclamp 700B (Axon Instruments). Data were recorded at 10 kHz, low pass filtered at 2 kHz and digitized with a Digidata 1440A digitizer (Axon Instruments). Borosilicate glass (Sutter Instruments Co., o.d. 1.5 mm, i.d. 0.86 mm) patch pipettes (3–8 MΩ) were pulled on a Flaming/Brown micropipette puller (Sutter Instrument Co.). The same mACSF was used as for the pipette solution. Data were acquired with pClamp and analysed in Matlab. Pneumatic electronic valves (Clippard Instruments) were used to control the flow of stimuli. Electronic valves were controlled via digital output from the Digidata 1440 A digitizer. The valves were opened for 20 s in every stimulated trial. For rat stimulus, we used 1:200 dilution of rat urine (male CD rats, Charles River, 2–6 months old) in mACSF. For ferret stimuli, ~50 ml volume of ferret bedding containing urine, faeces, fur and gland excretions was extracted with 50 ml of mACSF overnight at 4 °C, then filtered and used for experiments.

31. Miller, R. A. *et al.* Mouse (*Mus musculus*) stocks derived from tropical islands: new models for genetic analysis of life-history traits. *J. Zool.* **250,** 95–104 (2000).
32. Schaeren-Wiemers, N. & Gerfin-Moser, A. A single protocol to detect transcripts of various types and expression levels in neural tissue and cultured cells: in situ hybridization using digoxigenin-labelled cRNA probes. *Histochemistry* **100,** 431–440 (1993).
33. Danciger, E., Mettling, C., Vidal, M., Morris, R. & Margolis, F. Olfactory marker protein gene: its structure and olfactory neuron-specific expression in transgenic mice. *Proc. Natl Acad. Sci. USA* **86,** 8565–8569 (1989).